*Antarctic Science 24(1), 45–58 (2012)* © Antarctic Science Ltd 2011 doi:10.1017/S0954102011000599

# Magnetic fabric and tectonic setting of the Early to Middle Jurassic felsic dykes at Pitt Point and Mount Reece, eastern Graham Land, Antarctica

JIŘÍ ŽÁK[1,2], IGOR SOEJONO[2], VOJTĚCH JANOUŠEK[2,3] and ZDENĚK VENERA[2]

[1]*Institute of Geology and Palaeontology, Faculty of Science, Charles University, Albertov 6, Prague 12843, Czech Republic*
[2]*Czech Geological Survey, Klárov 3, Prague 11821, Czech Republic*
[3]*Institute of Petrology and Structural Geology, Charles University, Faculty of Science, Albertov 6, Prague 12843, Czech Republic*
*jirizak@natur.cuni.cz*

**Abstract:** At Pitt Point, the east coast of Graham Land (Antarctic Peninsula), the Early to Middle Jurassic (Toarcian–Aalenian) rhyolite dykes form two coevally emplaced NNE–SSW and E–W trending sets. The nearly perpendicular dyke sets define a large-scale chocolate-tablet structure, implying biaxial principal extension in the WNW–ESE and N–S directions. Along the nearby north-eastern slope of Mount Reece, the WNW–ESE set locally dominates suggesting variations in the direction and amount of extension. Magnetic fabric in the dykes, revealed using the anisotropy of magnetic susceptibility (AMS) method, indicates dip-parallel to dip-oblique (?upward) magma flow. The dykes are interpreted as representing sub-volcanic feeder zones above a felsic magma source. The dyke emplacement was synchronous with the initial stages of the Weddell Sea opening during Gondwana break-up, but it remains unclear whether it was driven by regional stress field, local stress field above a larger plutonic body, or by an interaction of both.

Received 25 February 2011, accepted 27 June 2011, first published online 23 September 2011

**Key words:** Anisotropy of magnetic susceptibility (AMS), Antarctic peninsula, Chon Aike silicic large igneous province, Gondwana break-up, regional extension, Trinity Peninsula Group

## Introduction

Examining internal fabric in dykes, isolated or in swarms, has provided a valuable source of information on magma flow directions, growth history of dyke-hosting fractures, and principal axes of regional extension during dyke emplacement (e.g. Le Gall *et al*. 2005). Moreover, analysis of the internal dyke fabric may help to reveal the location of magma source underneath the radiating dyke swarms in large igneous provinces (e.g. Ernst & Baragar 1992). In the upper crust, dykes are commonly fine-grained to aphanitic owing to their fast cooling rates (hours to days) and the direct observation of their fabric and internal structures is in many cases difficult. The fabric orientations and gradients are thus most commonly inferred using the anisotropy of magnetic susceptibility (AMS; Tarling & Hrouda 1993, see Borradaile & Jackson 2010 for a recent review), which yields orientation of magnetic lineation (the long axis of the AMS ellipsoid) and magnetic foliation (plane normal to the short axis of the AMS ellipsoid). This approach is, however, not straightforward as there is a variety of possibilities of how the AMS principal axes may relate to the shape-preferred orientation of mineral grains and to the overall dyke geometry, direction of magma flow, or deformation regime associated with the dyke opening (e.g. Rochette *et al*. 1999, Geoffroy *et al*. 2002, Cañón-Tapia 2004, Chadima *et al*. 2009).

This paper examines felsic dykes superbly exposed in two areas on opposite sides of the Victory Glacier, east coast of the Graham Land, north-eastern Antarctic Peninsula (Fig. 1a): at the Pitt Point outcrop, which is a nearshore deglaciated flat surface *c.* 2 x 2 km, and along the north-eastern slope of Mount Reece (Fig. 1b). The dykes allow for direct observation of contact relationships against the metamorphic host rock, flow banding and effects of its synmagmatic deformation. The field observations are then combined with the AMS data in order to interpret the dyke emplacement mode and magma flow directions. Finally, we infer the possible regional tectonic setting of the dykes and discuss some broader implications for the geometry of crustal extension linked to the early stages of the south-western Gondwana break-up and the mid-Jurassic formation of the Larsen Basin (north-western Weddell Sea).

## Geological setting

The felsic dykes examined in this study are hosted in the Permian–Middle Triassic quartzose metasandstones, metagreywackes, and metapelites of the Trinity Peninsula Group (TPG; Smellie 1991). The tectonic setting of these turbidite siliciclastic successions remains unclear (fore-arc, trench-slope, or back-arc basins), but most studies concur in the interpretation that the TPG has been involved in the subduction-accretion complex along the proto-Pacific active margin of south-western Gondwana (e.g. Barbeau *et al*. 2010 and references therein). The TPG has been

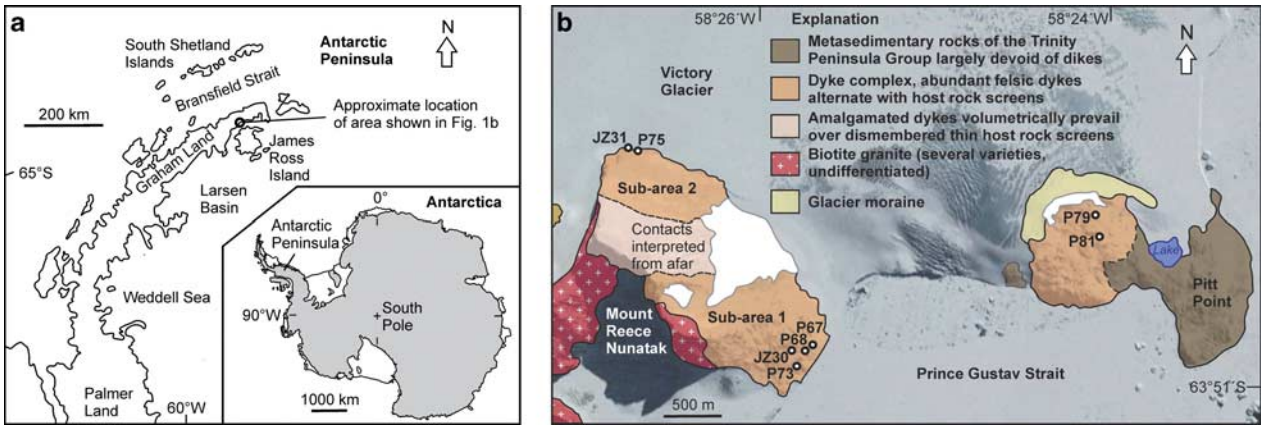


**Fig. 1.** Maps to show location and geology of the Pitt Point and Mount Reece areas. **a.** Greatly simplified outline of the northern Antarctic Peninsula (inset). The study area is located on the east coast of Graham Land. **b.** Simplified geologic map of the Pitt Point and Mount Reece areas (our new mapping, background image was taken from Google Maps, http://maps.google.cz/maps?hl=cs&ll=-63.834217,-58.451058&spn=0.036259,0.135441&t=f&z=13&ecpose=-63.83421688,-58.45105784, 7074.01,2.173,0,0&brcurrent=5,0,1, accessed November 2010). Inaccessible contacts were drawn from afar and thus their location and shape may not be accurate. Open circles indicate stations sampled for the AMS analysis.

affected by polyphase deformation and late Permian to early Triassic low-grade regional metamorphism under prehnite–pumpellyite to greenschist-facies conditions (Smellie *et al.* 1996, Wendt *et al.* 2008).

Some 30–35 km north-east along the coast from Pitt Point (in the Botany Bay–Camp Hill–Crystal Hill area), these basement rocks are overlain unconformably by the Lower to Middle Jurassic terrestrial, coal-bearing siliciclastic successions dominated by conglomerates and sandstones (Camp Hill Formation of the Botany Bay Group; Farquharson 1984). Samples from the Botany Bay Group dated using the U-Pb method on detrital zircons yielded maximum ages of deposition of 169 ± 1 Ma (Hunter *et al.* 2005) and 162–168 Ma (Barbeau *et al.* 2010). The Camp Hill Formation is devoid of volcanic rocks except for a single lapilli tuff horizon approximately in the middle of the succession, dated at 167 ± 1 Ma (U-Pb on zircons; Hunter *et al.* 2005). The Botany Bay sedimentary rocks were interpreted as having been deposited as debris flows, alluvial fans, and flood-plain deposits in relatively small fault-bounded basins (grabens) linked to the incipient lithospheric extension during the early stages of Gondwana break-up (Hathway 2000).

The siliciclastic rocks of the Camp Hill Formation are overlain conformably by subaerial volcanic rocks of chiefly rhyolitic and andesitic composition (formerly referred to as the Antarctic Peninsula Volcanic Group, recently redefined as the Graham Land Volcanic Group; Riley *et al.* 2010 and references therein). The volcanic rocks are dominated by ignimbrites and agglomerate tuffs. Lava flows, small domes, and sills are subordinate. At Camp Hill, U-Pb on zircons from an ignimbrite gave an age of 167 ± 2 Ma (Pankhurst *et al.* 2000). Elsewhere along the eastern coast of Graham Land, comparable volcanic rocks were dated at *c.* 162–171 Ma with the peak of igneous activity at *c.* 168 Ma (Riley *et al.* 2010).

In terms of lithology and field relationships, the felsic dykes examined in this study compare closely with the volcanic rocks found at Camp Hill and Crystal Hill. The Pitt Point and Mount Reece areas may thus expose a deeper, sub-volcanic section of now eroded volcanic apparatus, whereby the dykes may represent 'fossil' feeder zones (Riley & Leat 1999). The dykes are felsic, ranging from granite porphyry with feldspar and quartz phenocrysts up to 0.5 cm across to fine-grained or aphanitic rhyolite. They are all characterized by complex geometry and internal structures as described in great detail below. The new high-precision LA-ICP-MS zircon dating of these dykes yielded concordant U-Pb ages of 174.2 ± 0.6 Ma (2σ), 175.2 ± 0.7 Ma (Mount Reece), and 178.6 ± 0.7 Ma (Pitt Point), indicating the time span of dyke emplacement as *c.* 174–179 Ma (Early to Middle Jurassic; Janoušek & Gerdes unpublished data).

Further west, the TPG is intruded by a shallow-level granite pluton that makes up much of the Mount Reece nunatak. The pluton is composite and consists of several granite varieties. Perhaps the most widespread is a medium- to coarse-grained weakly porphyritic biotite granite. None of the granites displays evidence of syn-magmatic or sub-solidus deformation. The pluton/TPG contact is sharp, curviplanar or stepped and largely discordant to structures in the TPG. The emplacement of the granites thus clearly post-dated the low-grade metamorphism and regional deformation of the TPG. Field relationships indicate that the relative ages of the felsic dykes and the granite are more complex. The porphyritic biotite granite truncates the dyke complex in the pluton roof, but some rhyolite dykes also cross-cut a medium-grained equigranular schlieren-rich granite. This is consistent with the new geochronological data that indicate a prolonged granitic magmatism at Mount Reece (*c.*166–185 Ma; Janoušek & Gerdes, unpublished data).

https://doi.org/10.1017/S0954102011000599 Published online by Cambridge University Press

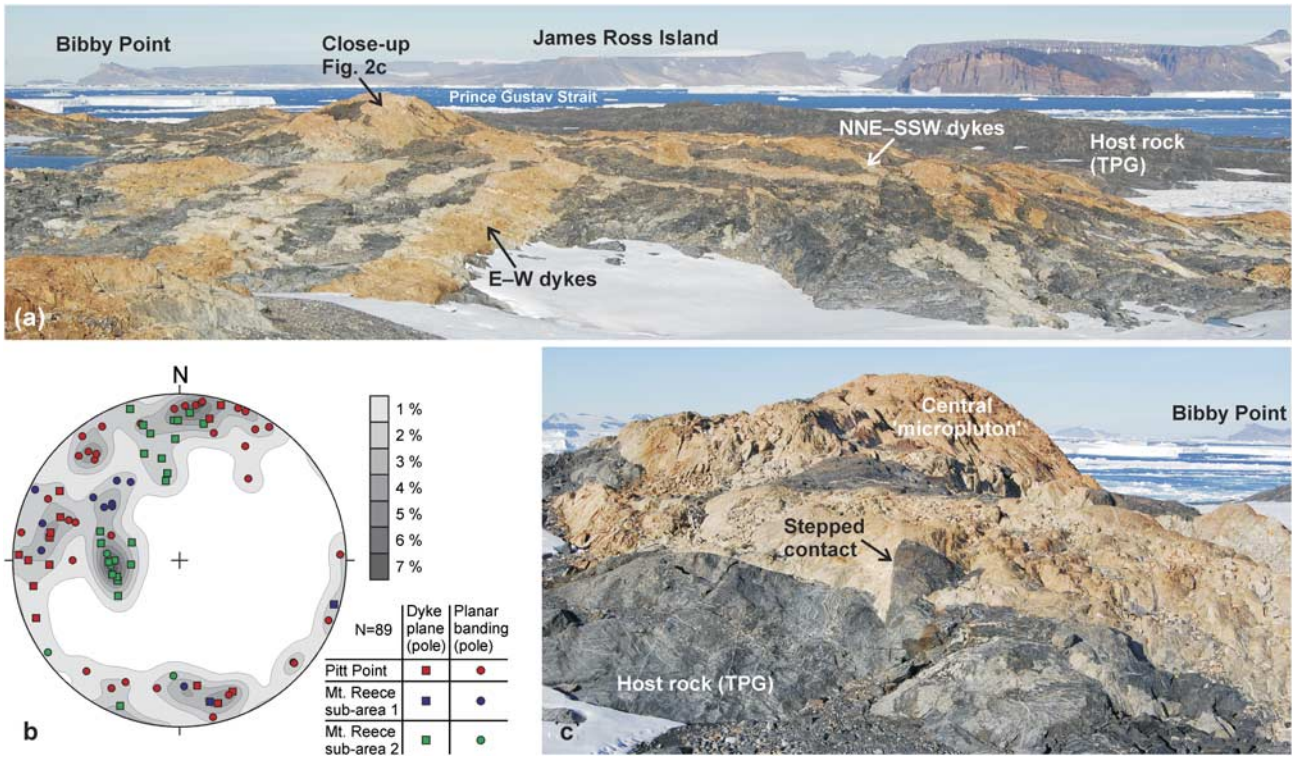


**Fig. 2.** Felsic dykes and associated structures in the Pitt Point area. **a.** Overview of the Pitt Point outcrop, looking east (approximately), towards the James Ross Island. Two perpendicular sets of felsic dykes are separated by thin host rock screens and merge in the central part of the outcrop. **b.** Stereonet (lower hemisphere, equal area projection) showing orientation of dyke planes and margin-parallel planar banding at Pitt Point and Mount Reece. **c.** Close-up of the central part of the Pitt Point outcrop where felsic dykes prevail over the host rock and coalesce to form a 'micropluton'. Note irregular, stepped contact defined by fractures at a high angle to each other. TPG = Trinity Peninsula Group.

## Field observations

### *Pitt Point*

The dykes exposed on the Pitt Point outcrop tend to form two sets oriented at a high angle to each other; one set strikes NNE–SSW and dips steeply to moderately to the ESE, the other set strikes E–W and dips steeply to the north or south (Fig. 2a & b). These two dyke sets define a network consisting of irregularly alternating domains where one set may dominate over the other. In the central part of the outcrop (Fig. 2a & c), the dyke rocks volumetrically prevail over the TPG host and dykes of both sets coalesce to form small (tens of metres across) intrusive bodies ('microplutons'). The TPG host rocks are here preserved only as elongated decimetre-thick screens (Fig. 3a) or more irregular, fracture-bounded blocks isolated between the dykes (Fig. 3b). Continuity of foliation across these blocks suggests that no rotation occurred during dyke emplacement.

The dyke/host contacts are knife-sharp fractures that truncate the pre-existing host rock structures (e.g. metamorphic foliation, compositional banding, minor folds; Fig. 3b). In detail, the contacts vary from straight to more irregular, but commonly are stepped, taking nearly 90° abrupt steps (Fig. 2c). In some cases, the dyke margins exhibit cuspate-lobate geometry with rhyolite cusps extending outward from a dyke into the host. The cusps are oriented at a high angle to the dyke margins and commonly are parallel to strike of the other complementary dyke set (Fig. 3c). Some dyke tips are blunt (Fig. 3d & e) and associated with complex arrays of shear fractures in the host rock.

No systematic cross-cutting relationships of the two dyke sets were observed. Instead, dykes of one set commonly pass into the other around a host rock 'corner', defined by two perpendicular dyke margins (Figs 2a & 3f). In some cases the E–W dykes cross-cut the NNE–SSW dykes (Fig. 3e & f), whereas in other cases cusps extending from margins of the E–W dykes taper toward the NNE (Fig. 3c). Relative temporal relationships of the dykes thus clearly indicate broadly contemporaneous propagation and emplacement of both sets.

Spectacular flow banding and magmatic folds are preserved in dykes of both sets. The banding is best seen on glacier-polished outcrops and is macroscopically defined by alternating light and dark bands (Fig. 4a & b). In the simplest cases, the alternating bands are planar and parallel to the dyke margins and have nearly constant

https://doi.org/10.1017/S0954102011000599 Published online by Cambridge University Press

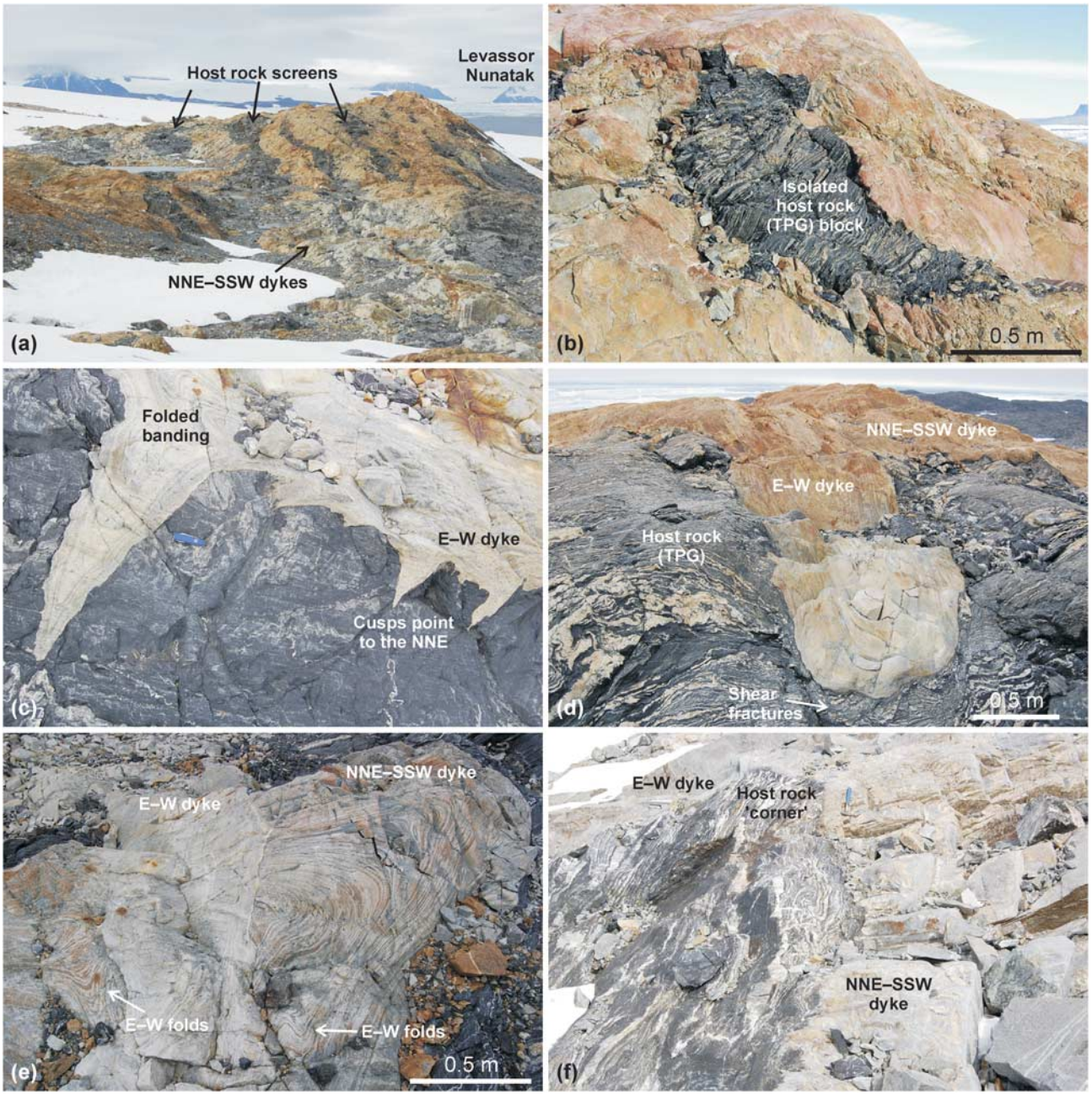


**Fig. 3.** Felsic dykes and associated structures in the Pitt Point area. **a.** The NNE–SSW dykes separated by thin host rocks screens, looking north-east (approximately). **b.** Close-up of a host rock block isolated within the dykes. Knife-sharp, discordant intrusive contacts truncate metamorphic foliation and quartz veins inside the block. **c.** Cusps extending towards the NNE from an E–W dyke. Note both the planar margin-parallel and folded flow banding in the dyke. Swiss Army knife (9 cm long) for scale. **d.** Close-up of blunt tip of an E–W dyke with minor shear fractures developed in the process zone near the dyke tip. **e.** An E–W dyke cutting across a NNE–SSW dyke, note magmatic folds having fold axial planes parallel to the younger dyke margin. **f.** Host rock 'corner' at the junction of two amalgamated nearly perpendicular dykes. Hammer for scale. TPG = Trinity Peninsula Group.

thickness along strike (Fig. 4c). More commonly, bands or their packages define variously-shaped magmatic folds showing no evidence of solid-state deformation. The folds are typically close to tight and have moderately to steeply plunging axes (Fig. 4d & e). However, in some cases more complex, irregular fold geometries are observed including rare sheath folds (Fig. 4f). Near the dyke margins, folds commonly follow contact irregularities, i.e. delineate contact steps or bulge into cusps (Figs 3c & 4e). Folded packages of individual bands are continuous for several

https://doi.org/10.1017/S0954102011000599 Published online by Cambridge University Press

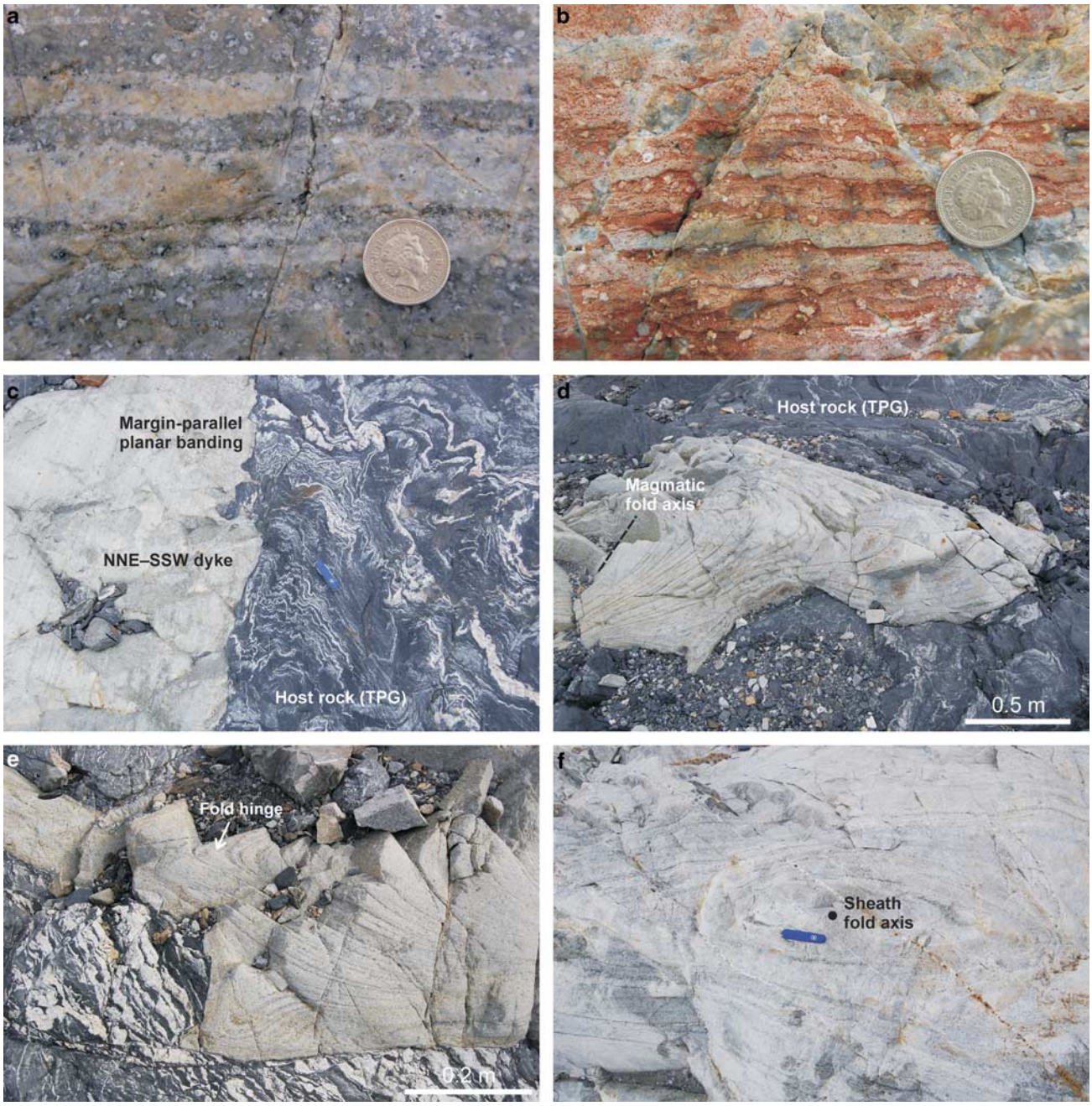


**Fig. 4.** Flow banding in dykes at Pitt Point. **a. & b.** Close-up of planar, margin-parallel flow banding defined by alternating pale and darker bands. **c.** Margin parallel layering in a NNE–SSW dyke, the contact truncates folded quartz veins in the host rock. Swiss Army penknife (9 cm long) for scale. **d. & e.** Flow banding folded into similar magmatic folds in which the individual bands thicken near the hinge regions and commonly pinch out away from the hinges. **f.** Nearly horizontal section (plan view) through a steep sheath fold defined by entirely enclosed flow banding. TPG = Trinity Peninsula Group.

metres within a dyke but also cross-cut or are detached from each other to form rootless folds. In contrast to the simple margin-parallel planar banding, the band thickness in folds may vary significantly. Both the light and dark bands attain the greatest thickness near the fold hinges, along the limbs their thickness decreases and the bands may pinch out (Fig. 4d & e).

*Mount Reece*

Along the north-eastern slope of Mount Reece, the felsic dykes were examined in two sub-areas, referred to as the sub-areas 1 and 2 in this paper (Fig. 1b). The sub-area 1 exposes predominantly steep NNE–SSW dykes similar to those at Pitt Point, while dykes in the sub-area 2 display

https://doi.org/10.1017/S0954102011000599 Published online by Cambridge University Press

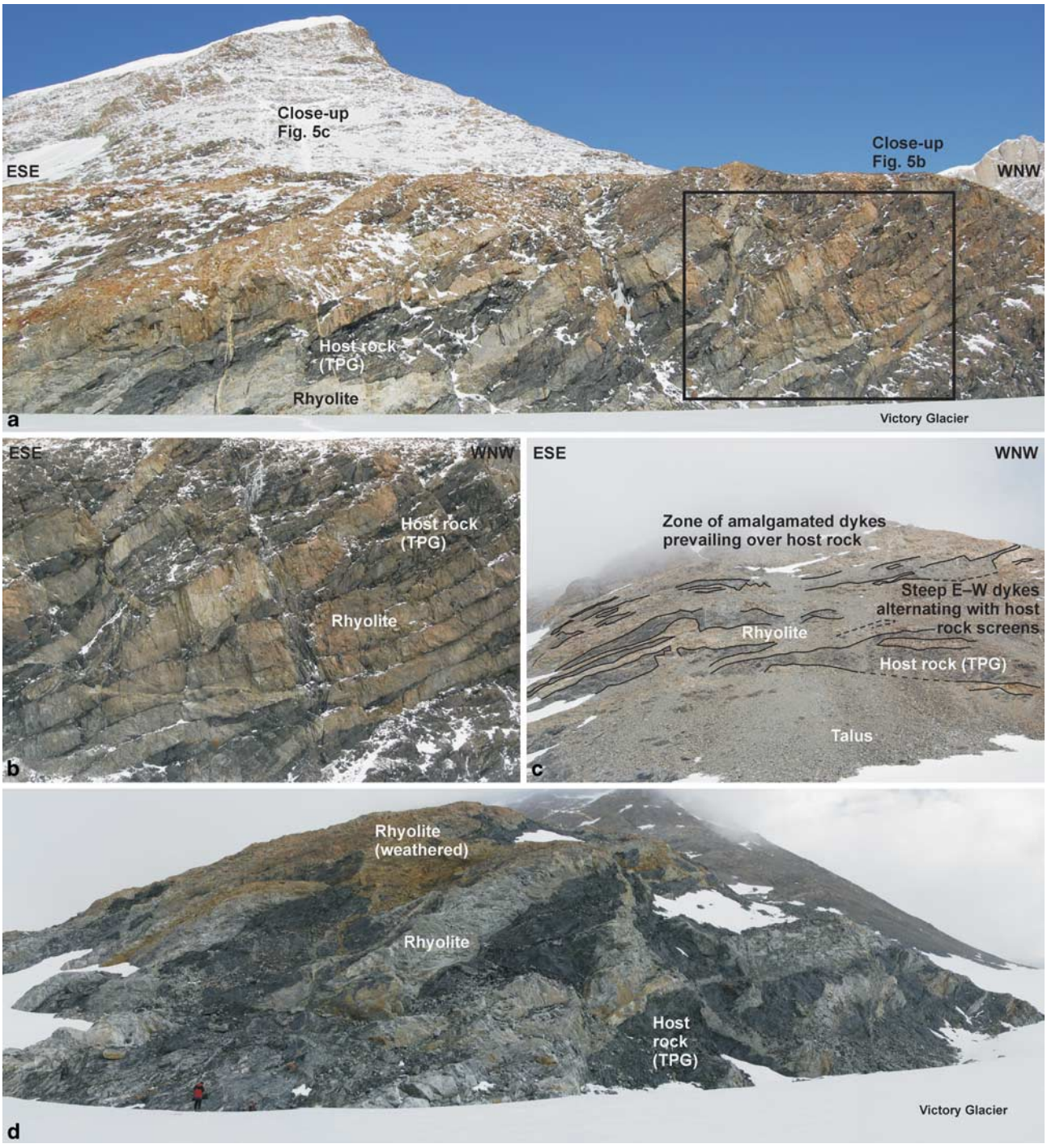


**Fig. 5.** Felsic dykes at the north-eastern slope of Mount Reece, sub-area 2. **a. & b.** Distant and close-up views on moderately dipping N–S dykes that intrude the metasedimentary rocks of the Trinity Peninsula Group (TPG) in the roof of a granite pluton, looking SSW (approximately). **c.** Steep E–W dykes alternating with abundant host rock screens pass upward into a zone of amalgamated dykes with only minor remnants of the host rock (largely obscured by clouds). **d.** Highly irregular host rock blocks disrupted and isolated by voluminous dykes.

two distinct orientations. One dyke set is specific to this area and strikes N–S and dips moderately to the East (Fig. 5a & b), the other set strikes E–W and dips steeply to moderately to the south (Fig. 5c). The dykes are generally voluminous (their thickness is up to several tens of metres and their along-strike length is up to several hundreds of metres) and roughly parallel and closely spaced (Fig. 5b). Thus much of the outcrop in the sub-area 2 is made up of

https://doi.org/10.1017/S0954102011000599 Published online by Cambridge University Press

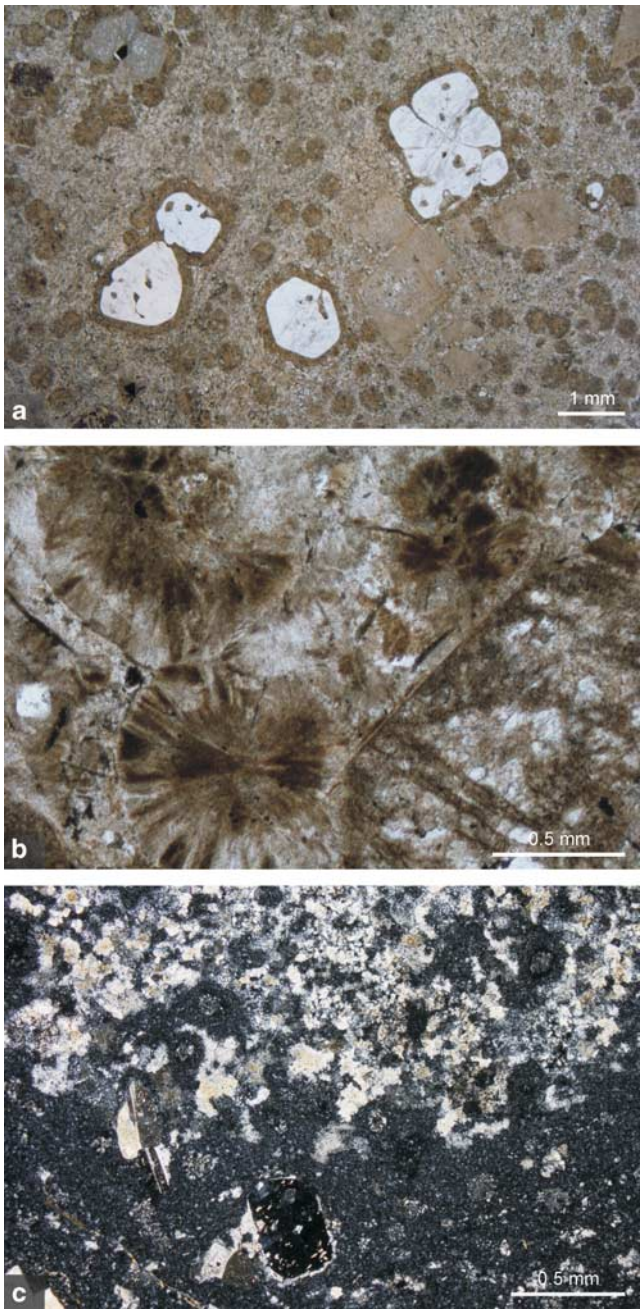


**Fig. 6.** Photomicrographs of the felsic dykes from the Pitt Point and Mount Reece areas. **a.** Spherulitic rhyolite enclosing rounded and variously embayed quartz phenocrysts. Mount Reece, sub-area 1 (plane-polarized light). **b.** Close-up of the spherules up to 1 mm across. Note the blade-shaped biotite crystals set in a very fine-grained matrix. Mount Reece, sub-area 2 (plane-polarized light). **c.** Contact between two adjacent bands of a flow-banded rhyolite. Mount Reece, sub-area 2. The upper band is holocrystalline and coarse grained, while the bottom band is very fine-grained, nearly isotropic with only a few phenocrysts. It most probably represents a relatively little devitrified glass (crossed polars).

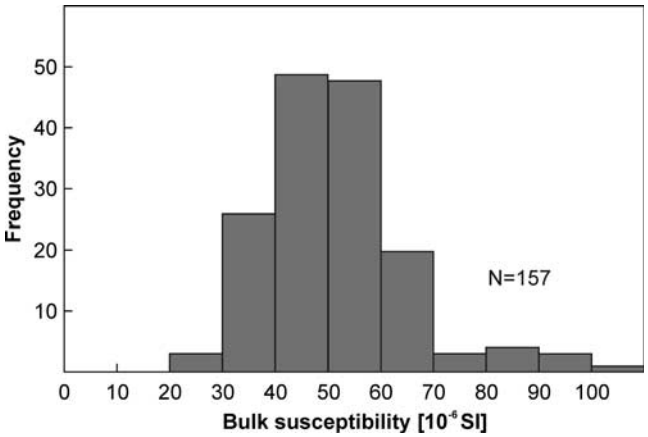


**Fig. 7.** Histogram of the bulk susceptibility distribution for all analysed specimens.

amalgamated dykes enclosing only thin, dismembered tabular screens or irregular blocks of the TPG host rock (Fig. 5). In detail, the dyke/host contacts are also knife-sharp and truncate minor structures (cleavage, compositional banding, and folds) in the metasedimentary host rocks. Flow banding is only locally developed along the dyke margins in comparison to abundant banding and magmatic folds in the dykes at Pitt Point.

## Microstructures

The felsic dykes at Pitt Point and Mount Reece show no evidence of subsolidus ductile deformation on either macroscopic or microscopic scales, and the textures are exclusively magmatic (see for example, the degree of preservation of the delicate spherules in Fig. 6a). The dykes are slightly porphyritic, felsic rocks (rhyolitic to microgranite) enclosing rounded, often strongly embayed quartz phenocrysts up to 4 mm in size (Fig. 6a). Phenocrysts of K-feldspar or plagioclase are scarce (the latter occur sporadically in glomerocrysts several millimetres across) and are contained in a fine-grained matrix enclosing numerous tiny bladed biotite crystals. Microgranitic, i.e. holocrystalline types, are relatively rare. Spherulitic textures are conspicuous with individual spherules 1.5–2 mm in diameter (Fig. 6a & b).

Under the microscope, it is evident that the different colour of individual bands in banded portions of the dykes is related to the variable grain size. The contacts between the adjacent bands are sharp in the field but serrated at the micro-scale. The presence of bands apparently reflects variable style of devitrification of the former glass (Fig. 6c), perhaps related to variable water contents (Seaman *et al*. 2009). On this basis the spherulites have most probably been generated from devitrified glass and not by the growth from rapidly crystallized, supercooled magma (see Hibbard 1995 and references therein).

https://doi.org/10.1017/S0954102011000599 Published online by Cambridge University Press

## Anisotropy of magnetic susceptibility (AMS)

Although AMS has been used extensively to examine 'cryptic' (magnetic) fabric patterns in igneous rocks (Hrouda 1982, Tarling & Hrouda 1993), only a few studies have applied this method in Antarctica (e.g. Dragoni *et al*. 1997, Curtis *et al*. 2008). In this paper, the AMS is used to complement our field observations and to describe quantitatively the orientation, symmetry, intensity, and gradients of magnetic fabric in the dykes.

### *Methodology*

Anisotropy of magnetic susceptibility is mathematically described as a symmetric second-rank tensor that relates the induced magnetization of a rock linearly with the intensity of an applied magnetic field, expressed through the equation:

$$M_i = k_{ij} H_j, \quad (1)$$

where $M_i$ (i = 1, 2, 3) are components of the magnetization vector, $H_j$ (j = 1, 2, 3) are components of the vector of intensity of applied magnetic field, and $k_{ij}$ are magnetic susceptibilities, i.e. dimensionless constants of proportionality (Hrouda 1982). The susceptibility tensor can be visualized as an ellipsoid. Its semi-axis lengths, $k_1 \geq k_2 \geq k_3$, are termed the principal susceptibilities and their orientations, $K_1$, $K_2$, $K_3$, the principal directions. Such an ellipsoid defines a magnetic fabric where the maximum direction ($K_1$) is denoted as magnetic lineation and the plane perpendicular to the minimum direction ($K_3$) and containing the maximum and intermediate directions ($K_1$, $K_2$) is magnetic foliation. The orientations of the principal susceptibilities are presented in stereograms (lower hemisphere, equal area projection) in the geographic co-ordinate system.

Anisotropy of magnetic susceptibility can be further characterized by several parameters (for a comprehensive list see Tarling & Hrouda 1993, pp 18 & 19). We use the mean magnetic susceptibility ($k_m$), degree of anisotropy (P), and shape parameter (T) defined as follows: $k_m = (k_1 + k_2 + k_3)/3$, $P = k_1/k_3$, and $T = 2\ln(k_2/k_3)/\ln(k_1/k_3) - 1$. The parameter $k_m$ represents the mean magnetic susceptibility, which reflects the type and volume fraction of magnetic minerals in the rock. The parameter P reflects the eccentricity of the AMS ellipsoid and may thus relate to the intensity of the preferred orientation of the magnetic minerals provided that the same AMS carriers are compared. The parameter T indicates the symmetry of the AMS ellipsoid; it varies from -1 (prolate AMS ellipsoid, i.e. perfectly linear magnetic fabric) through to 0 (triaxial AMS ellipsoid, i.e. transition between linear and planar magnetic fabric) to +1 (oblate AMS ellipsoid, i.e. perfectly planar magnetic fabric).

In this study, ten dykes were sampled at eight stations (Fig. 1b). Our strategy was to cover dykes of each set in the different sub-areas and also margins and centres within individual dykes where possible. In total, 14 oriented

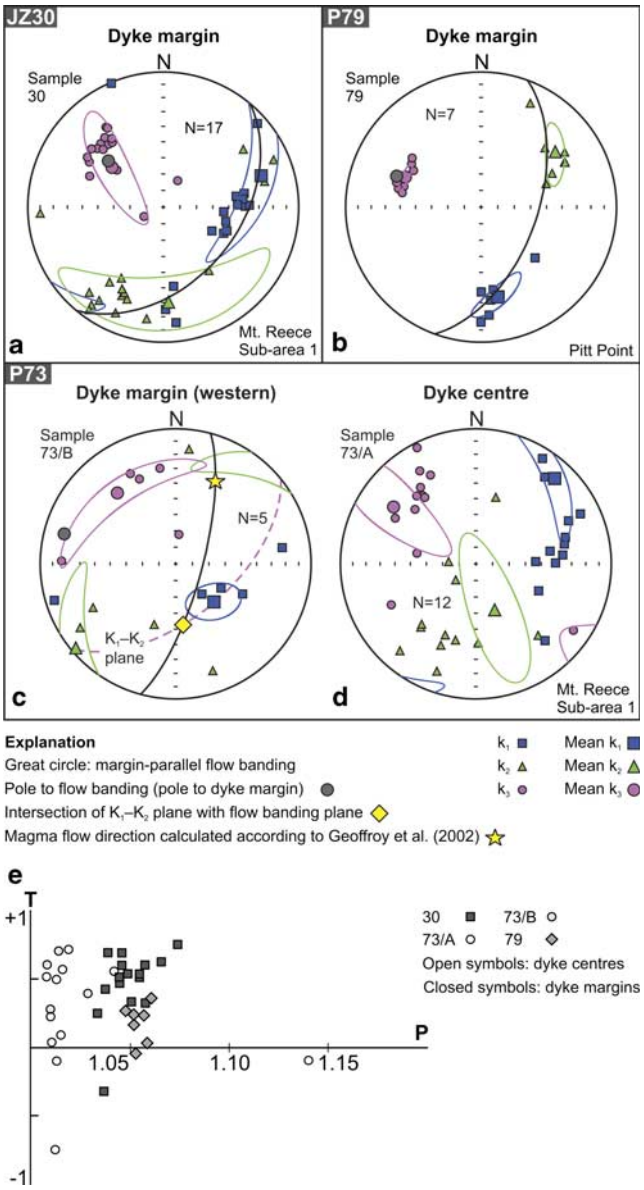


**Fig. 8. a.–d.** Stereographic projections (equal area, lower hemisphere) of the principal susceptibilities, and **e.** magnetic anisotropy P–T plot, from dykes that exhibit 'normal' fabric. See Fig. 1b for location of stations and the text for discussion.

blocks *c.* 20 x 20 x 15 cm in size (also referred to as samples in this paper) were hammered from the dykes. Two dykes were studied at Pitt Point (stations P79 and P81, one block from the margin of each dyke), four dykes in the sub-area 1 (one block from the margin of each dyke at stations JZ30 and P67, one block from the dyke centre at station P68, and one block from the dyke margin and one from the centre of the same dyke at station P73), and four dykes in the sub-area 2 (two dykes at station JZ31 with one block from the margin and one from the centre of each dyke, and two dykes at station P75 with one block from the margin and

https://doi.org/10.1017/S0954102011000599 Published online by Cambridge University Press

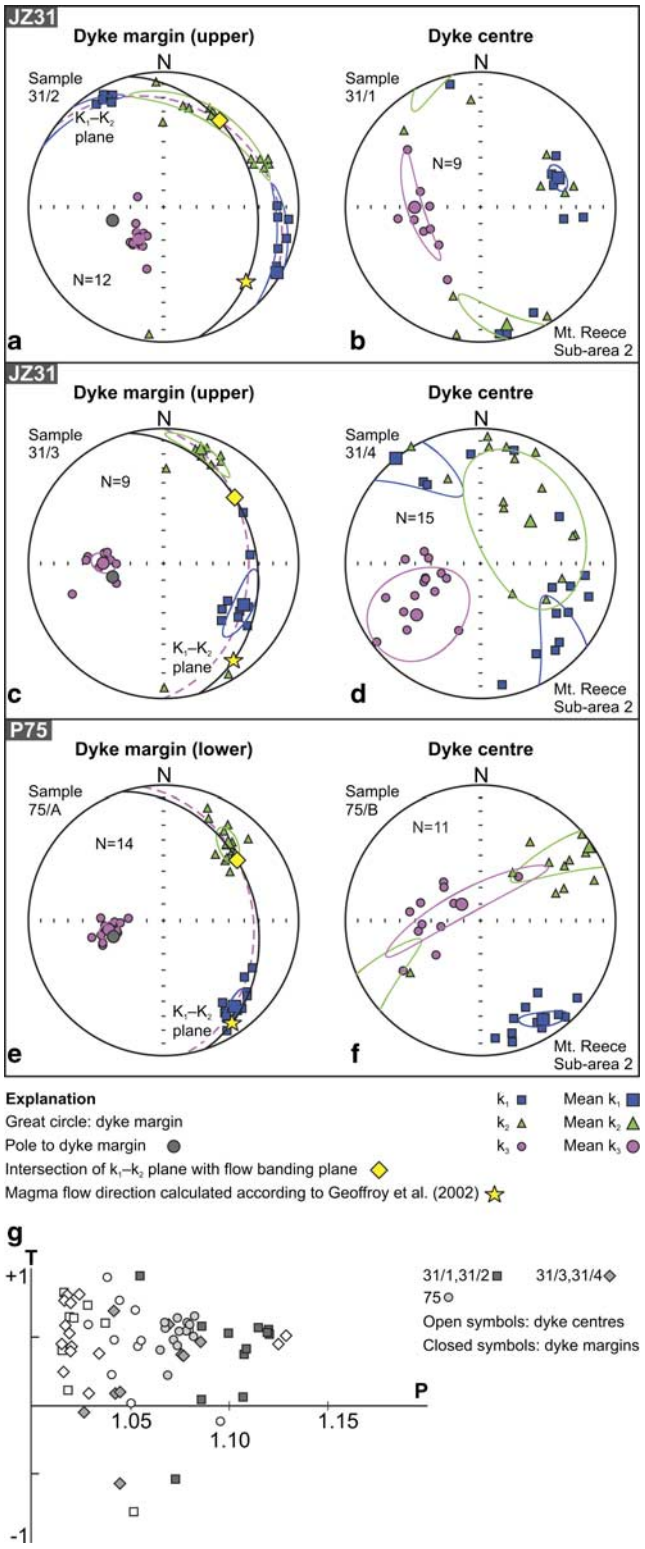


**Fig. 9. a.–f.** Stereographic projections (equal area, lower hemisphere) of the principal susceptibilities, and **g.** magnetic anisotropy P–T plot, of specimens from Mount Reece, sub-area 2. The dykes exhibit 'normal' fabric. See Fig. 1b for location of stations and the text for discussion.

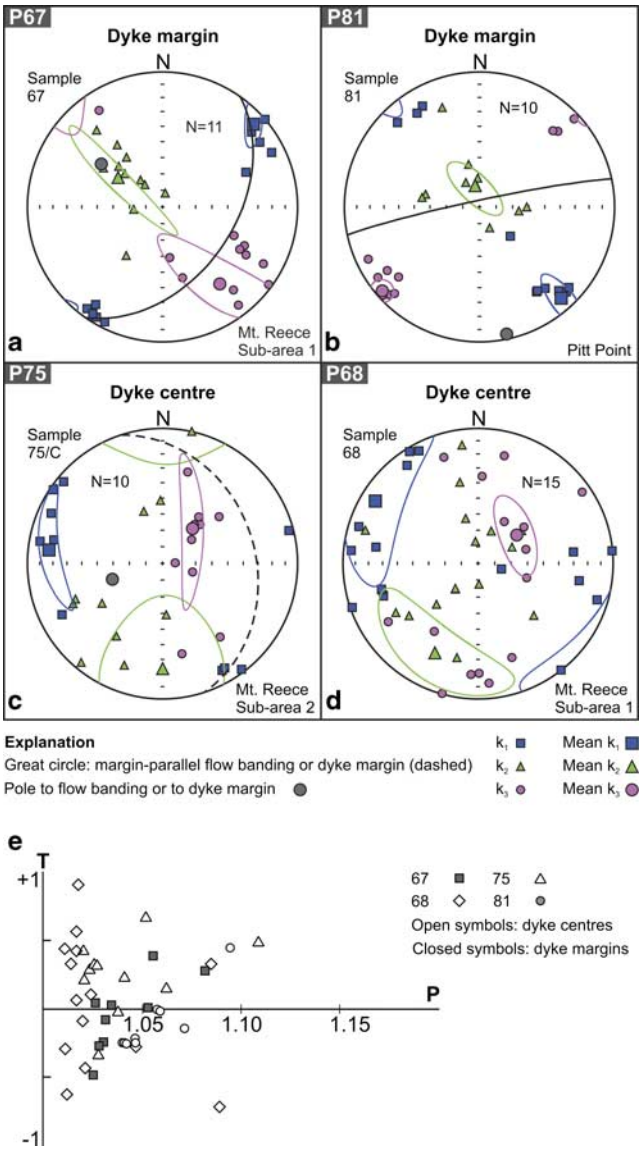


**Fig. 10. a.–d.** Stereographic projections (equal area, lower hemisphere) of the principal susceptibilities, and **e.** magnetic anisotropy P–T plot, of specimens that exhibit 'intermediate' (sample 67), 'inverse' (samples 81 and 75/C), and 'random' (sample 68) fabric. See Fig. 1b for location of stations and the text for discussion.

one from the centre of the same dyke and one block from the centre of another dyke). The blocks were then drilled in the laboratory, rotated back to their original (*in situ*) position, and the orientation of the drilled cores was measured using the standard orientation table. After cutting, the cores yielded 157 standard specimens (cylinder shaped, 2.1 cm high and 2.5 cm in diameter). The AMS was measured using a MFK1-A Spinner Kappabridge in the Laboratory of Rock Magnetism at the Institute of Geology and Palaeontology, Faculty of Science, Charles University in Prague. A statistical analysis of the AMS data was carried out using the ANISOFT package

https://doi.org/10.1017/S0954102011000599 Published online by Cambridge University Press

of programmes (the latest version written by Chadima & Jelínek; http://www.agico.com, accessed May 2008). The AMS data are listed in the electronic supplemental material to this article (http://dx.doi.org/10.1017/S0954102011000599) and presented in Figs 7–10. Orientations of the maximum, intermediate, and minimum principal susceptibilities in all specimens are plotted in geographic co-ordinates in a separate stereonet for each block (Figs 8–10; equal area projection, lower hemisphere).

### *Magnetic fabric parameters and orientation*

The bulk susceptibility of the analysed specimens is very low, of the order of $10^{-5}$ SI, and shows only slight variations with a pronounced maximum frequency of values between 40–60 x $10^{-6}$ SI (Fig. 7). Such low susceptibility values indicate that the AMS carriers are predominantly paramagnetic minerals (biotite) and that a significant contribution of ferromagnetic fraction can safely be excluded.

Magnetic fabric measured in the felsic dykes can be grouped into four types:

a) The first type, referred to as the 'normal' magnetic fabric (Rochette *et al*. 1992, 1999), is characterized by the minimum principal susceptibilities ($K_3$) clustered about the pole to the dyke margin (stations 30, 31, 73, 75, 79; Figs 8 & 9). That is, magnetic foliations ($K_1$–$K_2$ planes) are roughly parallel to the dyke plane and to the macroscopically discernible margin-parallel flow banding. In this case, both the magnetic lineations ($K_1$) and the intermediate principal susceptibilities ($K_2$) lay within or very close to the dyke/banding plane. The plunge of magnetic lineations varies from nearly down-dip (Figs 8c & 9b) through moderate (Figs 8a & 9d) to shallow (Figs 8b & 9a, e & f) and the $K_1$ and $K_2$ axes are distributed along the great circles of the margin-parallel flow banding in the stereonets. Several patterns of $K_1$ and $K_2$ can be further distinguished within the individual dykes. First, the $K_1$ and $K_2$ are clustered about their respective mean directions and have roughly the same orientation near the dyke margin and in the centre (samples 31/2–31/1 and 75/A–75/B; Fig. 9a & b and 9e & f). Second, the $K_1$ and $K_3$ axes are well clustered about the mean directions in the dyke centre but become more widely scattered near the margin maintaining roughly the same orientation (samples 31/3–31/4, respectively; Fig. 9c & d). Third, all the axes show greater spread about their mean directions and are slightly oblique to the dyke plane. That is, the $K_3$ axis is close to the pole of margin-parallel flow banding while the $K_1$ and $K_2$ axes lay near but not within the dyke plane (samples 73/B–73/A; Fig. 8c & d).

For the 'normal' fabric, the AMS ellipsoids are predominantly oblate (90% of the analysed specimens; Figs 8e & 9g) with the T parameter ranging from -0.778 to 0.945 (average T = 0.397). The P parameter scatters from 1.008–1.374, but the degree of anisotropy generally slightly increases from the dyke centres (average P = 1.049) towards the margins (average P = 1.062; Figs 8e & 9g).

b) The second type is the 'intermediate' fabric of Rochette *et al*. (1992, 1999), defined by the $K_2$ axes clustered about the pole to the dyke plane, $K_1$ axes plunging shallowly in the dyke plane, and $K_3$ axes close to the dyke plane (station 67; Fig. 10a). This fabric type is associated with the mostly prolate to neutral AMS ellipsoid (T = -0.482 to 0.671) and with the degree of anisotropy P = 1.027–1.032 for specimens with the prolate to neutral AMS ellipsoid and P = 1.027–1.386 for specimens with the oblate AMS ellipsoid (Fig. 10e).

c) The third type of fabric is 'inverse' (Rochette *et al*. 1992, 1999), that is the $K_1$ axes are perpendicular to the dyke plane while the remaining two axes lay close to ($K_2$) or at an angle ($K_3$) to the dyke plane (sample 75/C and station 81). At station 81 (Fig. 10b), the $K_2$ axes are steep and well clustered within the dyke plane and the $K_3$ axes are subhorizontal, associated with the mostly prolate AMS ellipsoid (T = -0.251 to 0.432) and with the P parameter ranging from 1.041–1.171 (Fig. 10e). In sample 75/C (Fig. 10c), the $K_2$ axes scatter widely about the trend of the dyke and the $K_3$ axes plunge steeply. These specimens yielded mostly oblate AMS ellipsoids (T = -0.328 to 0.662) and the degree of anisotropy from 1.020–1.109 (Fig. 10e).

d) The magnetic fabric from one dyke (station 68) is characterized by a wide scatter in the orientation of the principal susceptibilities (Fig. 10d) and by a wide range of shapes of the AMS ellipsoid (T parameter ranges from -0.702 to 0.986) for mostly very low degree of anisotropy (73% of specimens yielded P values $< 1.024$; Fig. 10e).

## Discussion

### *Interpretation of the AMS in the dykes*

In the simplest case of 'normal' magnetic fabric as revealed at stations JZ30 (Mount Reece, sub-area 1, NE–SW dyke) and P79 (Pitt Point, NNE–SSW dyke; Fig. 8a & b), magnetic foliations ($K_1K_2$ planes of the AMS ellipsoids) are subparallel to both the dyke plane and to the planar flow banding. Such a good agreement between the macroscopically determined planes and magnetic foliations indicates that the AMS ellipsoids mimic the fabric ellipsoids. Assuming the simplest relationship among the AMS, petrofabric, strain, and magma flow pattern, the magnetic lineations ($K_1$) and foliations ($K_1K_2$ planes) could be interpreted to represent principal stretching and planes normal to the principal shortening directions of the local strain ellipsoids, respectively, being parallel to the flow lines and flow planes of overall uniform laminar magma flow (Paterson *et al*. 1998). If this is correct, then the inferred magma flow directions are dip-oblique (stations JZ30, P79; Fig. 8a & b). In the absence of kinematic indicators, we can only assume that the magma flowed largely upwards.

At station P73 (Mount Reece, sub-area 1, NNE–SSW dyke), magnetic foliations are oblique to both the dyke

margin and margin-parallel flow banding (Fig. 8c). The interpretation of magma flow direction from the AMS is ambiguous in such a case: it could be either parallel to magnetic lineation or parallel to the dyke plane and perpendicular to the intersection of the dyke plane with magnetic foliation (Geoffroy *et al*. 2002; Fig. 8c).

The dykes from sub-area 2 at Mount Reece (stations JZ31 and P75; Fig. 9) generally lack flow banding and thus the relationship of the AMS to the internal dyke fabric is unclear. However, the flow directions inferred using the method of Geoffroy *et al*. (2002) are close to magnetic lineations in all cases (Fig. 9), suggesting mostly dip-oblique (?upward) magma flow. Unlike the parabolic, plug-like, or more complicated fabric and inferred magma flow patterns that have been reported from dykes, magnetic fabric in these dykes shows subtle across-dyke variations in the orientation of principal susceptibilities (Fig. 9a–f) while the P parameter is systematically elevated near the dyke margins (Fig. 9g, see also Fig. 8e). Given the very narrow range of the bulk susceptibility values (Fig. 7), the increase in the P parameter could be attributed to higher fabric intensity (and hence inferred strain) along dyke walls.

Although our AMS study was aimed at describing an overall fabric and inferred magma flow pattern on a larger-scale, it is interesting to note that the systematically elevated P parameter (Figs 8e & 9g) could imply that the development of planar banding was preferentially localized to higher P and higher strain zones near the dyke margins. In addition, we have shown that, where unaffected by syn-magmatic folding, the individual millimetre-scale bands: a) are planar and parallel to the dyke walls, b) can be traced for more than several metres distance, c) do not truncate each other, and d) maintain nearly constant thickness along their strike. These observations disprove the possibility of each layer representing a single magma pulse corresponding to a single fracture opening/magma injection event. In such a case, repeated magma injection during dyke opening would produce abundant 'scour-and-fill' truncations of individual layers and at least locally consistent younging (growth) directions, as described, for example, from mafic schlieren in granitoid plutons (e.g. Paterson 2009 and references therein). Recently, Seaman *et al*. (2009) proposed that similar flow banding in rhyolites formed by stretching of magma that contained zones of various water contents, leading subsequently to the development of alternating variously devitrified bands. This explanation is in concert with our field and microstructural observations and magnetic fabric study, the latter indicating that the banded dyke margins were more strained than the non-banded dyke interiors. After the banding had formed but before full solidification, the rhyolitic magma was still capable of flowing to produce a variety of small-scale magmatic folds (not examined in detail using the AMS; Fig. 4d & e).

A minority of the examined dykes (stations 67, 75, 81; Fig. 10) reveals other than 'normal' fabric types. The presence

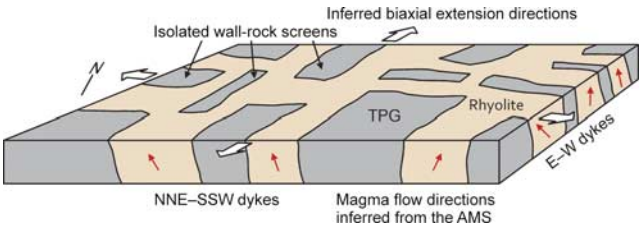


**Fig. 11.** Idealized sketch (not to scale) to show our structural interpretation of the Pitt Point outcrop where both coeval dyke sets are exposed and define a chocolate-tablet structure. The dip-parallel to dip-oblique (?upward) magma flow directions were inferred from the 'normal' magnetic fabric. Note that the amount and directions of extension, relative abundance of each dyke set, and the inferred magma flow directions may vary from one area to another; see the text for discussion. TPG = Trinity Peninsula Group.

of single-domain (SD) magnetite, which has been proposed to cause 'inverse' magnetic fabrics (e.g. Chadima *et al*. 2009), can be excluded because the bulk susceptibility is very low (Fig. 7). An alternative explanation is that the magnetic grains in these dykes aligned at a high angle to the overall magma flow direction, as a result of: a) divergent flow (Paterson *et al*. 1998), b) periodic fluctuations in particle orientations in general shear flow (e.g. Dragoni *et al*. 1997, Cañón-Tapia & Chávez-Álvarez 2004), c) compaction within already static magma (Hrouda *et al*. 2002), or d) increased grain interactions during late stage magma flow under decreasing magma pressure (Hastie *et al*. 2011). At station 68 (Fig. 10d), the principal susceptibilities scatter widely and are associated with a very low degree of anisotropy (Fig. 10e), perhaps reflecting a random to weak fabric in the dyke centre.

### *Implications for the Early to Middle Jurassic regional extension inboard of the palaeo-Pacific margin of Gondwana*

It has been widely accepted that the Lower to Middle Jurassic volcanic rocks of the Graham Land Volcanic Group record the incipient lithospheric extension that continued in the opening of the Weddell Sea (e.g. Riley & Leat 1999, Hathway 2000, Riley *et al*. 2010). These volcanic complexes have been correlated with the Middle Jurassic Chon Aike silicic large igneous province of Patagonia (Pankhurst *et al*. 1998) but also occur in a back-arc position with respect to the Antarctic Peninsula magmatic arc, which rimmed the palaeo-Pacific active margin of Gondwana (e.g. Leat *et al*. 1995, Hervé *et al*. 2007). Consequently, the driving forces for this lithospheric extension have been debated and it remains unclear whether the extension was triggered by a mantle plume (and is thus directly linked to the Gondwana break-up), by slab roll-back during eastward subduction of the palaeo-Pacific oceanic lithosphere, or by a combination of both.

https://doi.org/10.1017/S0954102011000599 Published online by Cambridge University Press

Although we are aware that it is difficult to extrapolate structural data from limited outcrop to a regional scale, our dyke fabric study may provide additional information on the style and geometry of the Early to Middle Jurassic lithospheric extension along the north-eastern coast of the Antarctic Peninsula. We have shown that at Pitt Point, the two perpendicular dyke sets emplaced at *c.* 174–179 Ma (Janoušek & Gerdes, unpublished data) are clearly coeval and define a chocolate-tablet structure (Figs 2a & 11). Assuming that the individual dykes opened perpendicular to the principal extension direction, as no evidence for major dyke-parallel shear component was observed, the deformation regime associated with the dyke emplacement is horizontal biaxial extension in the N–S and WNW–ESE directions (Fig. 11). Further west (at Mount Reece), such a prominent chocolate-tablet dyke network has not been observed and dykes of one set always prevail over the other (Fig. 5a & c) or show shallower dip than elsewhere (Fig. 5b) suggesting that the magma supply and the amount of extension in these particular directions may have locally varied. Although some uncertainty exists in the interpretation of magma flow directions as discussed above, our AMS data point to nearly dip-parallel to dip-oblique magma flow supporting the interpretation that the Mount Reece and Pitt Point dykes represent eroded sub-volcanic feeder zones above a magma source; their volcanic correlatives are common along the east coast of the Antarctic Peninsula (Riley & Leat 1999).

The above described structural pattern could be interpreted in two ways.

1) It is interesting to note that the dykes described in this paper are similar in their orientation distribution to the basaltic dykes reported from western Dronning Maud Land. Here, Riley *et al*. (2005) documented ENE–WSW dykes emplaced at *c.* 190 Ma and NNE–SSW dykes emplaced at *c.* 178 Ma. Moreover, Curtis *et al*. (2008) described more variably oriented dykes, but inferred two approximately perpendicular principal extension directions (NE–SW and NW–SE). Considering the almost identical radiometric age and similar orientation of the dykes, it is tempting to speculate that the extension documented at Pitt Point and Mount Reece could, at least in part, have resulted from a similar type of plume-related stress field to that driving the Early Jurassic extension in western Dronning Maud Land at *c.* 176–178 Ma. However, large post-Middle Jurassic plate rotations have been inferred for the Antarctic Peninsula and Weddell Sea regions on the basis of palaeomagnetic data (Grunow 1993, Elliot & Flemming 2000), and current palaeogeographic reconstructions indicate that the two areas were widely separated before the Gondwana break-up. At Graham Land's distance from the inferred plume offshore Dronning Maud Land, magma flow would have to be horizontal to be part of the same magma system. The above points thus rule out any reasonable comparison of the Graham Land and Dronning Maud Land dykes other than age.

2) More probably, the extension documented at Pitt Point and Mount Reece could have been driven by a complex interaction of a local stress field, resulting from an ascending or inflating magma body of a much larger size than are the dimensions of our study area, with the regional stress field related to the opening of the Weddell Sea. Indeed, the presence of low-density (?granitoid) rocks below the present-day erosion level is indirectly supported by a pronounced negative gravity anomaly in the Pitt Point–Mount Reece area, as revealed by a recent airborne gravity survey (Jordan *et al*. 2009). In addition, structures in the TPG host rock indicate ductile flow and hydrothermal activity associated with the north–south principal extension direction, presumably preceding intrusion of a granitoid body (Lexa & Venera, unpublished data). It can be inferred that the two sets of approximately perpendicular dykes may have been simultaneously emplaced in a domain of local interference between the regional stress field characterized by the east–west principal extension direction and the local stress field (associated with the north–south principal extension direction) above a presumed granitoid intrusion at depth.

## Conclusions

At Pitt Point, the Early to Middle Jurassic (Toarcian–Aalenian) steep rhyolite dykes form two nearly perpendicular sets (NNE–SSW and E–W). These two sets were emplaced simultaneously and define a large-scale chocolate-tablet structure, implying biaxial principal extension in WNW–ESE and N–S directions. At Mount Reece, the WNW–ESE set locally dominates, suggesting variations in the direction and amount of extension. Magnetic fabric in the dykes is predominantly 'normal' (the maximum and minimum principal susceptibilities lay within the dyke plane) and indicates dip-parallel to dip-oblique (?upward) magma flow. All the above is consistent with the dykes representing sub-volcanic feeder zones above a magma source. The dyke emplacement was synchronous with the onset of opening of the Weddell Sea, but it remains unclear whether it was driven by regional stress field, local stress field above a larger plutonic body, or by an interaction of both.

## Acknowledgements

We gratefully acknowledge Mike Curtis and Edgardo Cañón-Tapia for their constructive and thoughtful reviews and Alan Vaughan for careful editorial handling of this manuscript. We also thank Nick Halls for indispensable logistic support during the fieldwork, Ondrej Lexa for discussions and collaboration during the 2008 field season, and other colleagues from both 2008 and 2009 Czech expeditions for tolerating our group of geologists. The staff at Marambio are thanked for their hospitality and support. Marta Chlupáčová is thanked for help with the interpretation of magnetic mineralogy, Matěj Machek helped significantly

with drilling the AMS samples in the laboratory of the Institute of Geophysics of the Academy of Sciences of the Czech Republic. This research was funded by the Czech Geological Survey and Ministry of Environment of the Czech Republic through the Research Project No. SPII1a9/23/07 (to P. Mixa) and by the Ministry of Education, Youth and Sports of the Czech Republic through the Research Plan No. MSM0021620855.

## Supplemental material

A supplemental table will be found at http://dx.doi.org/10.1017/S0954102011000599.

## References

Barbeau, D.L., Davis, J.T., Murray, K.E., Valencia, V., Gehrels, G.E., Zahid, K.M. & Gombosi, D.J. 2010. Detrital-zircon geochronology of the metasedimentary rocks of north-western Graham Land. *Antarctic Science*, **22**, 65–78.

Borradaile, G.J. & Jackson, M. 2010. Structural geology, petrofabrics and magnetic fabrics (AMS, AARM, AIRM). *Journal of Structural Geology*, **32**, 1519–1551.

Cañón-Tapia, E. 2004. Anisotropy of magnetic susceptibility of lava flows and dykes: a historical account. *In* Martín-Hernández, F., Lüneburg, C.M., Aubourg, C. & Jackson, M., *eds. Magnetic fabric: methods and applications. Special Publication of the Geological Society of London*, No. 238, 205–225.

Cañón-Tapia, E. & Chávez-Álvarez, M.J. 2004. Theoretical aspects of particle movement in flowing magma: implication for the anisotropy of magnetic susceptibility of dykes and lava flows. *In* Martín-Hernández, F., Lüneburg, C.M., Aubourg, C. & Jackson, M., *eds. Magnetic fabric: methods and applications. Special Publication of the Geological Society of London*, No. 238, 227–249.

Chadima, M., Cajz, V. & Týcová, P. 2009. On the interpretation of normal and inverse magnetic fabric in dikes: examples from the Eger Graben, NW Bohemian Massif. *Tectonophysics*, **466**, 47–63.

Curtis, M.L., Riley, T.R., Owens, W.H., Leat, P.T. & Duncan, R.A. 2008. The form, distribution and anisotropy of magnetic susceptibility of Jurassic dykes in H.U. Sverdrupfjella, Dronning Maud Land, Antarctica. Implications for dyke swarm emplacement. *Journal of Structural Geology*, **30**, 1429–1447.

Dragoni, M., Lanza, R. & Tallarico, A. 1997. Magnetic anisotropy produced by magma flow: theoretical model and experimental data from Ferrar dolerite sills (Antarctica). *Geophysical Journal International*, **128**, 230–240.

Elliot, D.H. & Flemming, T.H. 2000. Weddell triple junction: the principal focus of Ferrar and Karoo magmatism during initial breakup of Gondwana. *Geology*, **28**, 539–542.

Ernst, R.E. & Baragar, W.R.A. 1992. Evidence from magnetic fabric for the flow pattern of magma in the Mackenzie giant radiating dyke swarm. *Nature*, **356**, 511–513.

Farquharson, G.W. 1984. Late Mesozoic, non-marine conglomeratic sequences of northern Antarctic Peninsula (the Botany Bay Group). *British Antarctic Survey Bulletin*, No. 65, 1–32.

Geoffroy, L., Callot, J.P., Aubourg, C. & Moreira, M. 2002. Magnetic and plagioclase linear fabric discrepancy in dykes: a new way to define the flow vector using magnetic foliation. *Terra Nova*, **14**, 183–190.

Grunow, A.M. 1993. Creation and destruction of Weddell Sea floor in the Jurassic. *Geology*, **21**, 647–650.

Hastie, W.W., Aubourg, C. & Watkeys, M.K. 2011. When an 'inverse' fabric is not inverse: an integrated AMS–SPO study in MORB-like dykes. *Terra Nova*, **23**, 49–55.

Hathway, B. 2000. Continental rift to back-arc basin: Jurassic–Cretaceous stratigraphical and structural evolution of the Larsen Basin, Antarctic Peninsula. *Journal of the Geological Society*, **157**, 417–432.

Hervé, F., Pankhurst, R.J., Fanning, C.M., Calderón, M. & Yaxley, G.M. 2007. The South Patagonian batholith: 150 my of granite magmatism on a plate margin. *Lithos*, **97**, 373–394.

Hibbard, M.J. 1995. *Petrography to petrogenesis*. Upper Saddle River, NJ: Prentice Hall, 587 pp.

Hrouda, F. 1982. Magnetic anisotropy of rocks and its application in geology and geophysics. *Geophysical Surveys*, **5**, 37–82.

Hrouda, F., Chlupáčová, M. & Novák, J.K. 2002. Variations in magnetic anisotropy and opaque mineralogy along a kilometer deep profile within a vertical dyke of the syenogranite porphyry at Cínovec (Czech Republic). *Journal of Volcanology and Geothermal Research*, **113**, 37–47.

Hunter, M.A., Cantrill, D.J., Flowerdew, M.J. & Millar, I.L. 2005. Mid-Jurassic age for the Botany Bay Group: implications for Weddell Sea Basin creation and southern hemisphere biostratigraphy. *Journal of the Geological Society*, **162**, 745–748.

Jordan, T.A., Ferraccioli, F., Jones, P.C., Smellie, J.L., Ghidella, M. & Corr, H. 2009. Airborne gravity reveals interior of Antarctic volcano. *Physics of the Earth and Planetary Interiors*, **175**, 127–136.

Leat, P.T., Scarrow, J.H. & Millar, I.L. 1995. On the Antarctic Peninsula batholith. *Geological Magazine*, **132**, 399–412.

Le Gall, B., Tshoso, G., Dyment, J., Kampunzu, A.B., Jourdan, F., Féraud, G., Bertrand, H., Aubourg, C. & Vétel, W. 2005. The Okavango giant mafic dyke swarm (NE Botswana): its structural significance within the Karoo Large Igneous Province. *Journal of Structural Geology*, **27**, 2234–2255.

Pankhurst, R.J., Riley, T.R., Fanning, C.M. & Kelley, S.P. 2000. Episodic silicic volcanism in Patagonia and the Antarctic Peninsula: chronology of magmatism associated with the break-up of Gondwana. *Journal of Petrology*, **41**, 605–625.

Pankhurst, R.J., Leat, P.T., Sruoga, P., Rapela, C.W., Marquez, M., Storey, B.C. & Riley, T.R. 1998. The Chon Aike province of Patagonia and related rocks in West Antarctica: a silicic large igneous province. *Journal of Volcanology and Geothermal Research*, **81**, 113–136.

Paterson, S.R. 2009. Magmatic tubes, pipes, troughs, diapirs, and plumes: late-stage convective instabilities resulting in compositional diversity and permeable networks in crystal-rich magmas of the Tuolumne batholith, Sierra Nevada, California. *Geosphere*, **5**, 496–527.

Paterson, S.R., Fowler, T.K., Schmidt, K.L., Yoshinobu, A.S., Yuan, E.S. & Miller, R.B. 1998. Interpreting magmatic fabric patterns in plutons. *Lithos*, **44**, 53–82.

Riley, T.R. & Leat, P.T. 1999. Large volume silicic volcanism along the proto-Pacific margin of Gondwana: lithological and stratigraphical investigations from the Antarctic Peninsula. *Geological Magazine*, **136**, 1–16.

Riley, T.R., Flowerdew, M.J., Hunter, M.A. & Whitehouse, M.J. 2010. Middle Jurassic rhyolite volcanism of eastern Graham Land, Antarctic Peninsula: age correlations and stratigraphic relationships. *Geological Magazine*, **147**, 581–595.

Riley, T.R., Leat, P.T., Curtis, M.L., Millar, I.L., Duncan, R.A. & Fazel, A. 2005. Early–Middle Jurassic dolerite dykes from western Dronning Maud Land (Antarctica): identifying mantle sources in the Karoo Large Igneous Province. *Journal of Petrology*, **46**, 1489–1524.

Rochette, P., Aubourg, C. & Perrin, M. 1999. Is this magnetic fabric normal? A review and case studies in volcanic formations. *Tectonophysics*, **307**, 219–234.

Rochette, P., Jackson, M. & Aubourg, C. 1992. Rock magnetism and the interpretation of anisotropy of magnetic susceptibility. *Reviews of Geophysics*, **30**, 209–226.

SEAMAN, S.J., DYAR, M.D. & MARINKOVIC, N. 2009. The effects of heterogeneity in magma water concentration on the development of flow banding and spherulites in rhyolitic lava. *Journal of Volcanology and Geothermal Research*, **183**, 157–169.

SMELLIE, J.L. 1991. Stratigraphy, provenance and tectonic setting of (?)Late Palaeozoic–Triassic sedimentary sequences in northern Graham Land and South Scotia Ridge. *In* THOMSON, M.R.A., CRAME, J.A. & THOMSON, J.W., *eds*. *Geological evolution of Antarctica*. Cambridge: Cambridge University Press, 411–417.

SMELLIE, J.L., ROBERTS, B. & HIRONS, S.R. 1996. Very low and low-grade metamorphism in the Trinity Peninsula Group (Permo–Triassic) of northern Graham Land, Antarctic Peninsula. *Geological Magazine*, **133**, 583–594.

TARLING, D.H. & HROUDA, F. 1993. *The magnetic anisotropy of rocks*. London: Chapman and Hall, 217 pp.

WENDT, A.S., VAUGHAN, A.P.M. & TATE, A. 2008. Metamorphic rocks in the Antarctic Peninsula region. *Geological Magazine*, **145**, 655–676.